Check for updates

EurJOC
European Journal of Organic Chemistry

Chemistry Europe
European Chemical Societies Publishing

Accepted Article

Title: A mechanism for selective recognition of cyanide in organic and aqueous solution: nucleophilic aromatic substitution of hydrogen and occurring biologically important benzisoxazole

Authors: Ergin Keleş, Burcu Aydıner, Yahya Nural, Nurgül Seferoğlu, Ertan Şahin, and Zeynel Seferoğlu

This manuscript has been accepted after peer review and appears as an Accepted Article online prior to editing, proofing, and formal publication of the final Version of Record (VoR). This work is currently citable by using the Digital Object Identifier (DOI) given below. The VoR will be published online in Early View as soon as possible and may be different to this Accepted Article as a result of editing. Readers should obtain the VoR from the journal website shown below when it is published to ensure accuracy of information. The authors are responsible for the content of this Accepted Article.

To be cited as: *Eur. J. Org. Chem.* 10.1002/ejoc.202000342

Link to VoR: https://doi.org/10.1002/ejoc.202000342

WILEY-VCH

10.1002/ejoc.202000342

WILEY-VCH

FULL PAPER

A new mechanism for selective recognition of cyanide in organic and aqueous solution: cyanide-induced nucleophilic aromatic substitution of hydrogen (NASH) and occurring biologically important benzisoxazole

Ergin Keleş[a], Burcu Aydıner[a], Yahya Nural[b,c], Nurgül Seferoğlu[d], Ertan Şahin[e] and Zeynel Seferoğlu*[a]

[a] E. Keleş, Assoc. Prof. Dr. B. Aydıner, Prof. Dr. Z. Seferoğlu
Gazi University, Department of Chemistry, 06560, Ankara, Turkey. Tel.: +90 312 2021525. E-mail: znseferoglu@gazi.edu.tr (Z.SEFEROĞLU).
http://w3.gazi.edu.tr/~znseferoglu/index.html
[b] Assoc. Prof. Dr. Y. Nural
Department of Analytical Chemistry, Faculty of Pharmacy, Mersin University, 33169, Mersin, Turkey
[c] Advanced Technology, Research and Application Center, Mersin University, 33343 Mersin, Turkey
[d] Prof. Dr. N. Seferoğlu
Department of Advanced Technology, Gazi University, 06560 Ankara, Turkey
[e] Prof. Dr. E. Şahin
Department of Chemistry, Faculty of Science, Atatürk University, 25240, Erzurum, Turkey

Supporting information for this article is given via a link at the end of the document.

Abstract: A simple colorimetric and fluorimetric chemosensor 3,5-dinitro-(*N*-phenyl)benzamide (**DNBA**), was synthesized for selective determination of cyanide anion in organic and aqueous solutions via novel chemodosimeter approach. The chemosensor **DNBA** showed a chromogenic and fluorogenic selective response to CN^- against competing anions such as F^-, AcO^- and $H_2PO_4^-$ in organic (DMSO and ACN) and in aqueous solutions (in DMSO/H_2O: 8/2, v/v). A mechanism between **DNBA** and cyanide which was named as aromatic substitution of cyanide to the dinitrophenyl ring via abstraction of hydrogen was presented. The intensive colorimetric and fluorimetric color changes were observed in ambient light and UV-light (λ_{ex}. 365 nm) after cyanide interacted with **DNBA**. To explain colorimetric and fluorimetric changes that comes from dominantly the cyanide addition to dinitrophenyl ring in **DNBA**, *N*-methyl-3,5-dinitro-*N*-phenylbenzamide (**DNBAM**) was synthesized. A method that can be used in the synthesis of new biologically active benzisoxazole compound was described by the reaction of **DNBA** with TBACN and KCN in DMSO or DMSO/H_2O, respectively. All interaction mechanisms between **DNBA** and cyanide and fluoride anions were demonstrated by experimental studies using various spectroscopic methods such as UV-vis, fluorescence, $^1H/^{13}C$ NMR and mass spectrometry as well as X-ray diffraction method. In addition, the experimental results were also explained with theoretical data. The spectroscopic results showed that cyanide interacts with three different mechanisms named as deprotonation, nucleophilic aromatic substitution, and formation of benzisoxazole ring. In addition, **DNBA** has lower LOD (Limit of detection) than WHO (World Health Organization) value for the detection of cyanide.

Introduction

The colorimetric and fluorimetric chemosensor for sensing anions have attracted much interest as a result of being applied in detecting hazardous anions, observation of enzyme reactions associated with anions, and bioimaging of anions.[1] In addition, single molecular optical probes that can sense multiple anions or cations have become of great significance due to simultaneous analysis of these analytes, which may surmount the challenges encountered with loading multiple indicators.[2] In the past decades, various anions have been found to play an important role in the advancement of dental health,[3] metabolic processes,[4] energy storage, and signal transduction systems.[5] Therefore, lots of efforts have been committed towards the design and development of new protocols and anion probes for the detection of fluoride, cyanide, acetate, etc., in the last decades. Fluoride is the most electronegative anion and it has strong hydrogen bonding ability with different probes having acidic -NH and -OH groups. Hence, many probes which have acidic proton have been developed for sensing fluoride.[6] In the meanwhile, to the detection of cyanide, many different strategies such as hydrogen bonding,[7] chemodosimeters,[8] displacement approaches[9] and addition mechanism[10] have been developed. In addition, various approaches in sensing cyanide anion have been formulated to enhance the sensitivity, selectivity, and dynamical working range recently.[11] However, till now cyanide detection via nucleophilic aromatic substitution of cyanide to electron-deficient dinitroarenes has not been published.

DNBA has an amide functional group as the receptor part and can easily be synthesized by the well-known procedure.[12] Because of having acidic hydrogen on the amide functional group, it may be used as a simple colorimetric chemosensor for some important anions such as CN^-, F^-, AcO^-, $H_2PO_4^-$ etc. The anion sensitivity of **DNBA** towards some selected anions such as F^- and CN^- via deprotonated process or H-bonding interaction in acetonitrile (ACN) was published in a previous article.[12] In that article, the color changes were seen easily with the naked-eye after interaction of **DNBA** with CN^- and F^- from colorless to pink and yellow, respectively. However, color changes were not observed in methanol:H_2O (9:1) binary solvents. Interestingly, in that article both mechanisms were proposed using color change only in ambient-light. Herein, previously proposed mechanisms between **DNBA** and CN^- were improved and rebutted by using well-known spectroscopic methods such as UV-vis, fluorescence,

This article is protected by copyright. All rights reserved.

Accepted Manuscript

and ^{1}H NMR titration methods and mass spectrometry analysis as well as X-ray structural analysis technique. Besides, the deprotonation of amide proton, according to our proposed mechanism cyanide reacts with dinitrophenyl fragment via nucleophilic aromatic substitution of hydrogen (NASH). In addition, while isolating products, benzisoxazole ring formation was swiftly observed via ring closure reaction by cyano and nitro group in dicyano derivative of **DNBA**.[13]

For anion selectivity study, **DNBA** has interacted with ten selective anions (I^-, Br^-, Cl^-, F^-, CN^-, AcO^-, $H_2PO_4^-$, NO_3^-, $ClO4^-$, and $HSO4^-$) in organic solvents (DMSO and ACN) and aqueous solution (DMSO/H_2O: 8/2). While F^- interacted with **DNBA** via partial the deprotonated process or H-bonding interaction in ACN and DMSO, CN^- interacted with **DNBA** via the deprotonation process and nucleophilic aromatic substitution to the electron deficient dinitrophenyl fragment in ACN and DMSO, and also in aqueous solution. In addition, *N*-methyl-3,5-dinitro-*N*-phenylbenzamide (**DNBAM**) was synthesized for explain colorimetric and fluorimetric change that comes from dominantly the cyanide addition to dinitrophenyl ring in **DNBA**. **DNBA** for the detection of CN^- displayed a lower limit of detection (LODs) than the WHO value. Finally, proposed mechanisms were confirmed with theoretical calculations.

Results and Discussion

Preparation of DNBA, DNBAM, tricyano derivatives of DNBA and 3-amino-7-cyano-6-nitro-*N*-phenylbenzo[c]isoxazole-4-carboxamide (CN-2a). **DNBA** and **DNBAM** were obtained in good yields by reacting aniline and *N*-methylaniline with 3,5-dinitrobenzoyl chloride, respectively (**Scheme 1**). The structure of the both synthesized compounds was confirmed by FT-IR, ^{1}H/^{13}C-NMR and LCMS/HRMS spectroscopic techniques as well as elemental analysis (Supporting Information, **Figures S1-9**).

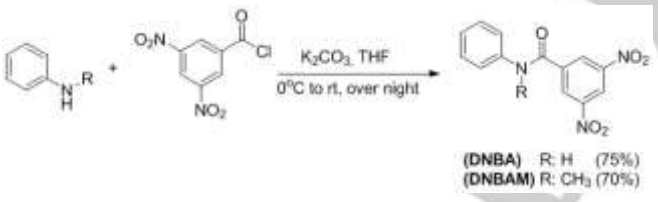

Scheme 1. Synthesis of **DNBA** and **DNBAM**.

To isolate mono, di- and tricyano substituted **DNBA** derivatives, many reactions were done in organic solvents and a binary solvent such as DMSO/H_2O. In these reactions, while monocyano and dicyano derivatives of **DNBA** could be not isolated, tricyano derivative was obtained in trace amounts (less than 1%) (Supporting Information, **Figure S9**) and it could be characterized only by ^{1}H NMR spectrum. However, the novel benzisoxazole compound **CN-2a** was obtained by ring closing reaction via dicyano derivatives of **DNBA** while isolating of the compounds from the crude product (**Scheme 2**).

Scheme 2. Synthesis of **CN-2a**.

The reactions for the synthesizing of the benzisoxazole derivative were performed in DMSO or DMSO-H_2O mixture using TBACN or KCN as a nucleophile source. When the synthesis of the benzisoxazole compound was performed by reaction of **DNBA** and 3.0 equiv KCN in DMSO or DMSO/H_2O for 96 h, the obtained yield is 3% and 8%, respectively. However, when 3.0 equiv TBACN was used as a cyanide source and the reaction was performed in DMSO, it was observed by TLC that the reaction was completed in two hours, and after flash chromatography, **CN-2a** was obtained in 35% yield. The structure of the **CN-2a** was fully characterized by single-crystal X-ray diffraction analysis (**Figure 1-2, and Table S1-5**) and other analytical techniques such as UV-vis and Fluorescence spectroscopy (Supporting Information, **Figures S10-19**). Even though 1.0, 2.0 or 3.0 equiv of TBACN or KCN were used in the reactions, nucleophilic addition products of mono or di-cyano substituted could not be observed in any isolated products. Moreover, when the reaction was performed by **DNBA** and 3.0 equiv TBACN, expected product as a result of triple nucleophilic aromatic substitution of the cyano group could not be isolated in a significant yield (less than 1%). When 3.0 equiv KCN used instead of TBACN, this product could not be observed. These results showed cyano group firstly bind to the ortho position (according to carbonyl) of the 3,5-dinitrophenyl and the second nucleophilic aromatic addition of cyanide is to the para position of the 3,5-dinitrophenyl ring. And then, the ring closing reaction was occurred by o-cyano and one of the nitro groups in the dinitrophenyl ring.

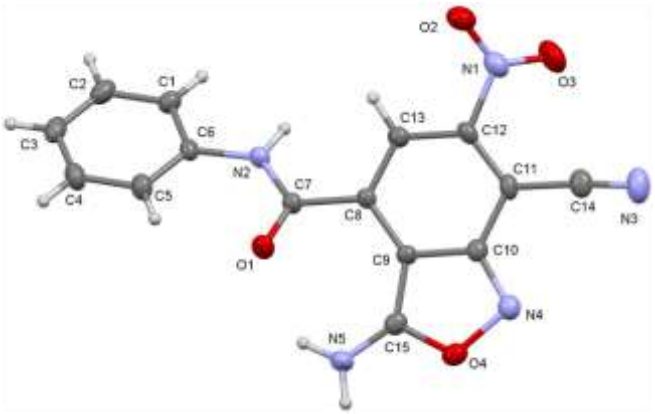

Figure 1. The crystal structure of **CN-2a** prepared via slow evaporation from a solution of ethyl acetate/n-hexane and analysed at 273 K (40% probability contours).

Accepted Manuscript

This article is protected by copyright. All rights reserved.

Anion interaction study in organic solvents

The selectivity of the various anions (I^-, Br^-, Cl^-, F^-, CN^-, AcO^-, $H_2PO_4^-$, NO_3^-, ClO_4^- and HSO_4^- with tetrabutylammonium as a counter cation) towards the chemosensor **DNBA** (*c* = 30 µM in DMSO) were examined. The chemosensor **DNBA** showed a selective chromogenic response to CN^- and F^-. The UV-vis and the fluorescence spectra were recorded in order to study the sensing abilities of the prepared **DNBA** in various concentrations and different mixture of solvents (organic and aqueous). **DNBA** is a colorless compound and it has no absorption band in the studied titration method in the range of 250-700 nm in DMSO or ACN and in DMSO/H_2O: 8/2 (v/v).

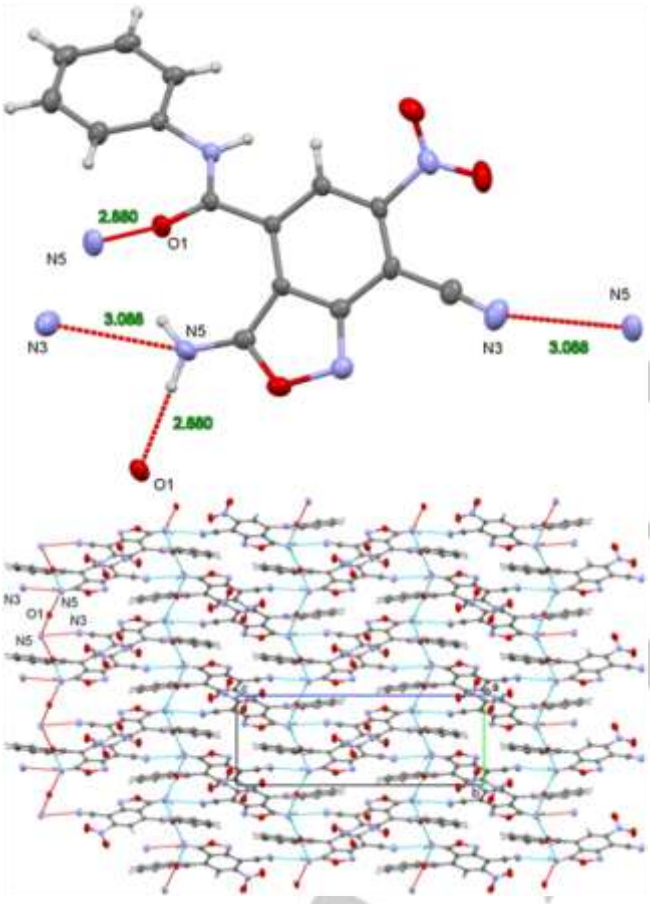

Figure 2. H-bonding geometry (up) and Stacking motif of **CN-2a** with the unit cell viewed down along the a-axis (down).

With respect to the UV-vis spectrum of **DNBA** (*c* = 30 µM), as depicted in **Figure 3a**, the addition of 20 equiv of F^- anion led to the appearance of a new dominant band at 313 nm and a broad weak band at 425 nm. The titration of **DNBA** with CN^- was studied by adding increasing concentrations of the anion. In addition, as can be seen in **Figure 3a**, upon addition cyanide to DMSO solution of **DNBA** the new three absorption bands with maxima were observed at 399, 550 and 627 nm. The absorption titration results show that **DNBA** interact with fluoride via partial deprotonation and hydrogen-bonding interaction processes (**Scheme 3**, **A** and **B**). However, the observed three absorption bands can be attributed to a different mechanism between cyanide and **DNBA**. While the observed short wavelength at 399 nm may be attributed mono cyanide addition to dinitrophenyl fragment, the longer wavelengths values at 550 and 627 nm may attributed di and tricyano addition, respectively. To attribute observed three absorption maxima in visible region and colorimetric and fluorimetric changes, same titration condition was applied between cyanide and **DNBAM** and almost same results were obtained. The results show that these observed absorption maxima and color changes can be attributed dominantly cyanide addition to dinitrophenyl ring (Supporting Information, **Figures S20**-**25**).

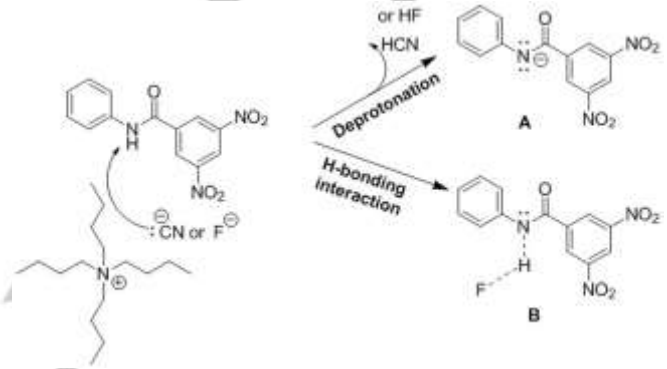

Scheme 3. Proposed deprotonation and hydrogen bonding mechanisms.

To determine the solvent effect on interaction study, DMSO was changed with ACN. While ACN was used instead of DMSO as a solvent, the almost same results were observed for cyanide addition (**Figure 3b**). However, there are some differences for fluoride addition in ACN. Fluoride has hygroscopic and strong hydrogen bonding properties in protic solvents. It has a strong base behavior especially in aprotic organic solvents that have no acidic proton such as DMSO, THF, ACN, etc. but it exhibits a weak base property in protic solvents such as methanol, water, etc.[14] In our proposed mechanism, fluoride removed a proton from ACN and occurred a carbanion from deprotonated ACN ($^-$:CH_2CN). The fluoride or $^-$:CH_2CN firstly removed a proton from amide and it was obtained deprotonated **DNBA**. Then, $^-$:CH_2CN attack to electron-deficient dinitrophenyl ring. Upon addition of 20 equiv of fluoride to **DNBA** solution (*c*= 30 µM) in ACN, the obtained lowest absorption band at 310 nm can be attributed to deprotonation of **DNBA** with $^-$:CH_2CN or fluoride. The wavelength observed in longer wavelength (at 395 and 617 nm in ACN, respectively) can be attributed to the mono or di addition of $^-$:CH_2CN to the dinitrophenyl fragment (**Scheme 4**). According to proposed mechanism, $^-$:CH_2CN bind to the both ortho positions (according to carbonyl) of the 3,5-dinitrophenyl because of steric hindrance of para position. These values are consistent with obtained absorption maxima values upon the addition of cyanide to **DNBA** in ACN.

The colorimetric and fluorimetric naked-eye detection of anions are very important for the applicability of the determination of anions in a real sample. While **DNBA** showed the change in coloration from colorless to purple for CN^-, light yellow color was

This article is protected by copyright. All rights reserved.

Accepted Manuscript

observed upon addition of 20 equiv of the fluoride anion. Meanwhile, the other competing anions (I^-, Br^-, Cl^-, NO_3^-, ClO_4^-, and HSO_4^-) did not show any color changes as can be seen in **Figure 3** (inset). These results indicated that **DNBA** can be used as a selective colorimetric sensor for colorimetric separation of fluoride and cyanide without any interference from other competitive anions. In addition, detailed mechanisms between cyanide/fluoride and **DNBA** were proved by using ^{1}H NMR and mass spectroscopic methods (see sensing mechanism part).

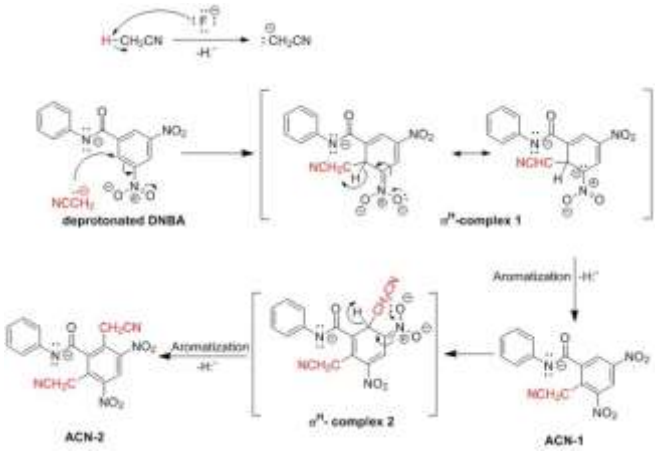

Scheme 4. Proposed mechanisms on acetonitrile addition to dinitrophenyl fragment in basic fluoride solution.

To explain the observed deprotonation, $^-$:CH_2CN and CN^- addition mechanism for both anions, a reversibility test was done. TFA was added to a solution of **DNBA**-F^- in ACN, in order to study the reversibility of the chemosensor. As depicted in **Figure 4a**, the addition of 100 equiv of TFA to a solution of **DNBA**-F^- with 20 equiv of TBAF led to a removal of the absorption band at 310 nm in the UV-vis spectra, and change in coloration of the solution from yellow to colorless. However, the intensities of absorbance at 395 nm and 617 nm wavelengths are still observed. These absorption maxima are attributed to addition of $^-$:CH_2CN to dinitrophenyl fragment and the plausible mechanism that can be seen in **Scheme 4**. However, after the addition of 100 equiv of TFA to a solution of **DNBA**-CN^-, it was only observed that the absorption bands of intensities at 400, 553 and 627 nm, were decreased because of partial protonation of the anionic intermediates such as Meisenheimer complex. Besides three absorption maxima, new absorption maximum was obtained in a shorter wavelength at 250 nm. It can be attributed to the protonation of the amide group (**Figure 4b**). These results supported that CN^- added to the dinitrophenyl fragment via nucleophilic aromatic substitution of hydrogen and they also showed that the interaction of **DNBA** with fluoride anion can be reversed by adding TFA in DMSO (**Scheme 3**).

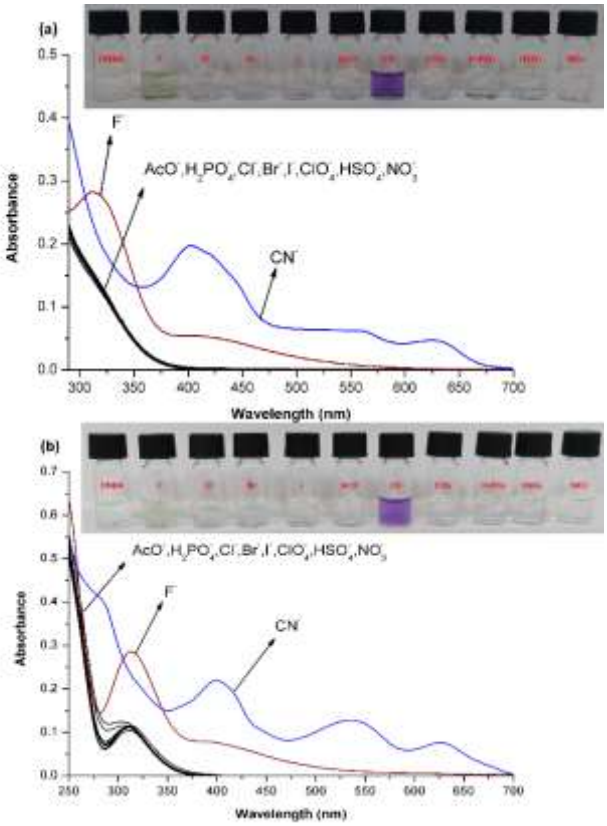

Figure 3. The absorption spectrum of **DNBA** (*c*= 30 µM), (a) in DMSO (b) in ACN after the addition of 20 equiv of all the anions. Insets: color changes after the addition of 20 equiv of anions.

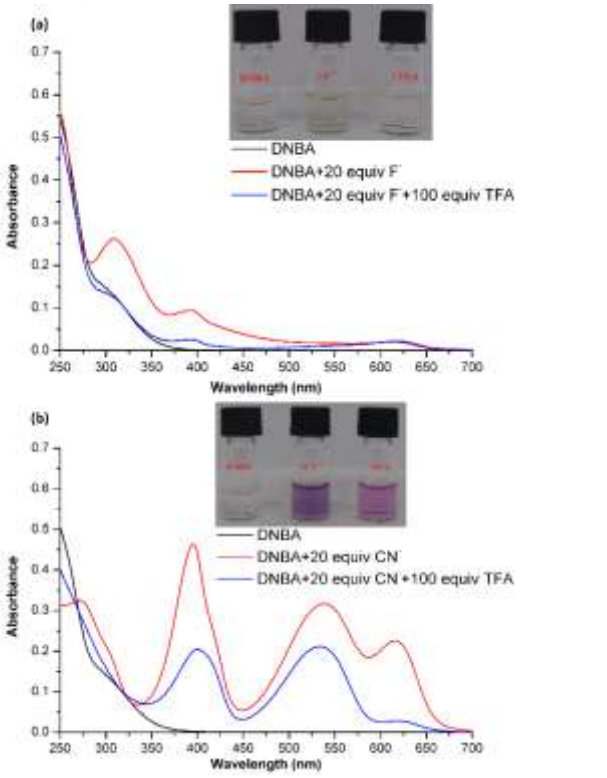

Figure 4. Absorption spectrum of **DNBA** (*c*= 30 µM, (a) upon addition 20 equiv of F^- and 100 equiv of TFA in ACN, respectively (b) upon the addition 20 equiv of CN^- and 100 equiv of TFA in ACN, respectively. Insets: color changes after the addition of 20 equiv of fluoride/cyanide and TFA, respectively.

This article is protected by copyright. All rights reserved.

Accepted Manuscript

DNBA is almost non-fluorescence in DMSO. However, the emission spectrum of the interaction of **DNBA** with CN^- anion showed the existence of a new dominant band at 671 nm with a shoulder at around 605 nm and also a weak band was observed at 468 nm. As can be seen in **Figure 5**, only CN^- responded towards **DNBA** in DMSO, while the remaining anions did not show any appreciable change in the spectral properties, even fluoride that interacted with **DNBA** in DMSO via deprotonation of the amide functional group. The color of the solution became red under UV irradiation ($\lambda_{ex.}$ 365 nm) after the addition of 10 equiv of CN^- anion as shown in **Figure 5** (inset). This result shows that deprotonation does not affect observed emission. The same titration was applied between cyanide and **DNBAM** and almost same results were obtained (Supporting Information, **Figures S22-25**).

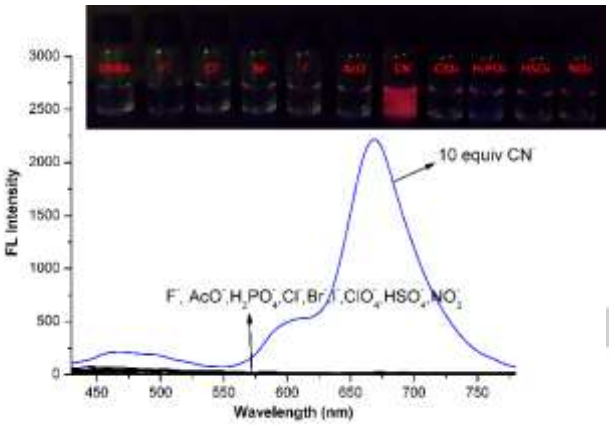

Figure 5. The emission spectrum of **DNBA** (*c*= 30 µM in DMSO) after the addition of 10 equiv of all the anions. Insets: fluorescence color changes after the addition of 10 equiv of cyanide under UV lamp ($\lambda_{ex.}$ 365 nm).

As seen from **Figure 6**, upon the addition of 20 equiv of CN^- to a solution of **DNBA**, the new emission band at 670 nm was increased. After excess addition (from 25 to 85 equiv) of cyanide anion, the emission band decreased and new band in a shorter wavelength at 468 nm appeared (red-colored lines). Interestingly, while the same conditions applied for fluoride anion, fluorescence changing was not observed in DMSO (**Figure 5**). As shown in **Fig. 6-inset** under UV irradiation ($\lambda_{ex.}$ 365 nm), while upon addition of 20 equiv of CN^- the color of the solution became red, upon addition of 85 equiv of CN^- the color of the solution changed as green. It shows that cyanide adds to the dinitrophenyl fragment through a few steps such as mono, di and tricyano addition. However, when ACN was used instead of DMSO, both anions showed fluorescence enhancement. While, after cyanide interacts with **DNBA**, the same emission curves were observed in ACN, different colors were obtained (**Figures 7** and **8**). The obtained data from fluorescence titration studies showed that the increasing fluorescence can be attributed to the addition of cyanide (for cyanide addition) and $^-$:CH_2CN (for fluoride addition) to the dinitrophenyl fragment, respectively (**Schemes 4** and **6**).

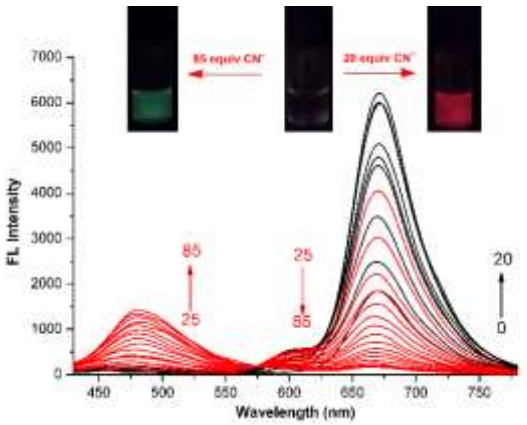

Figure 6. The emission spectrum of **DNBA** (*c*= 30 µM in DMSO) after the addition of 85 equiv of cyanide anion. Insets: fluorescence color changes after the addition of 85 equiv of cyanide under UV lamp ($\lambda_{ex.}$ 365 nm).

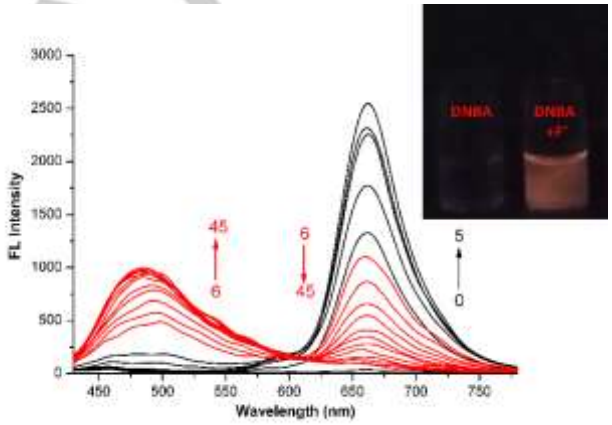

Figure 7. The emission spectrum of **DNBA** (*c*= 30 µM in ACN) upon the addition of 45 equiv of F^- in ACN under UV lamp ($\lambda_{ex.}$ 365 nm).

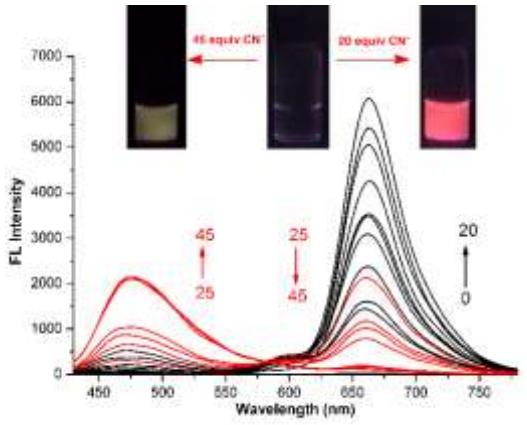

Figure 8. The emission spectrum of **DNBA** (*c*= 30 µM in ACN) upon the addition of 45 equiv of CN^- in ACN under UV lamp ($\lambda_{ex.}$ 365 nm).

Accepted Manuscript

This article is protected by copyright. All rights reserved.

Sensing Mechanism Study of DNBA

The mechanism of nucleophilic aromatic substitution of cyanide to the dinitrophenyl fragment and the deprotonation or hydrogen bonding interaction with fluoride were determined by ^{1}H NMR titration method in DMSO-d_6. At first, **DNBA** (c= 10 mM) was titrated with F^- (up to 2 equiv) in DMSO-d_6. As seen from **Figure 9** and **Scheme 5**, after the addition of fluoride, the phenyl protons (H_4, H_5, and H_6) and H_1 were shifted slightly to the upper field. These small shifts (Δδ≈0.24) and the broadband at 16.04 ppm indicated that an amide -NH is completely deprotonated but has a strong interaction with fluoride via hydrogen bonding interaction.

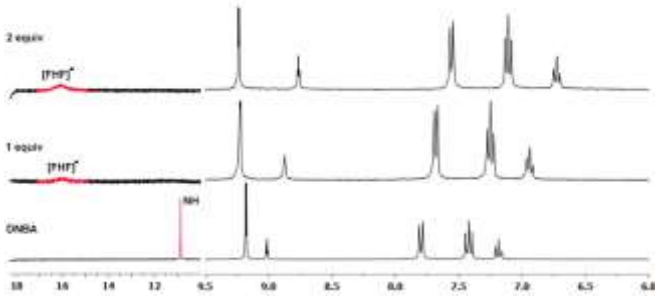

Figure 9. Partial ^{1}H-NMR spectral change of DNBA (c= 10 mM) with titration of TBAF (c= 1 M) in DMSO-d_6.

After the interaction mechanism of the fluoride was determined, the DMSO-d_6 solution of **DNBA** (c= 10 mM) was titrated with CN^- up to 2 equiv. As seen from **Figure 10**, upon the addition of 0.25 equiv of CN^-, the new signals began to appear. While the blue colored ones were easily determined as deprotonation products in which cyanide acts as a base, new signals at the lower field (10.07 and 9.76 ppm) and upper field (5.67 and 5.41 ppm) indicated that there was another process at the same time. The orange and the cyan colored signals at the upper field were defined as **σ^H-adduct** as intermediate. This result show that cyanide may be attacked to simultaneously the ortho and para position of dinitrophenyl ring (**Schemes 5** and **6**).

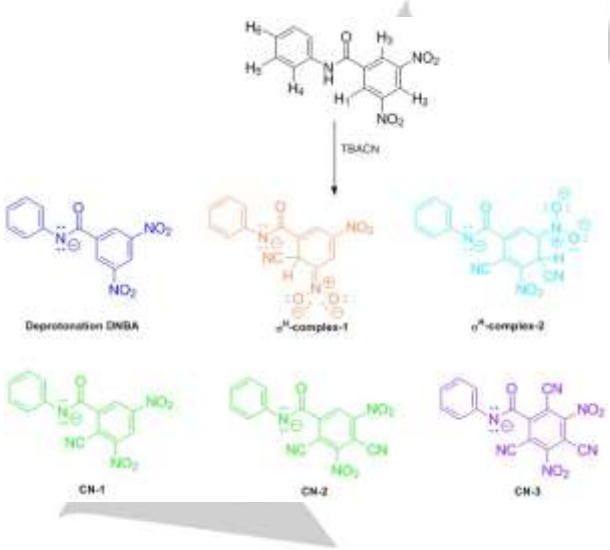

Scheme 5. Proposed intermediates during cyanide titration of **DNBA**.

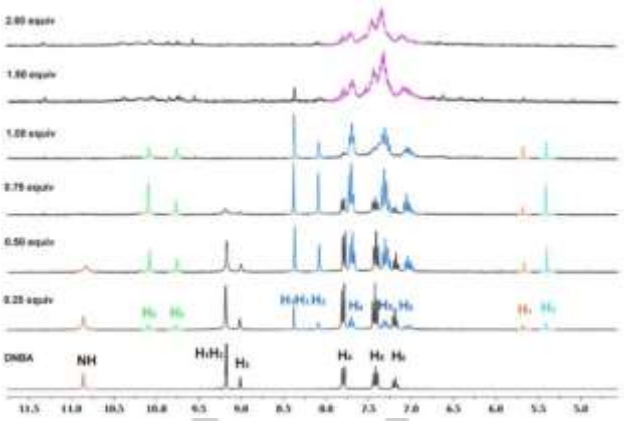

Figure 10. Partial ^{1}H-NMR spectral change of **DNBA** (c= 10 mM) with titration of TBACN (c= 1 M) in DMSO-d_6.

When titration was continued to 1 equiv of cyanide, the deprotonation process was completed as black colored signals that belong to **DNBA** and -NH signal disappeared. All these changes at signals suggest that two different mechanisms such as deprotonation and addition began at the same time but at the end of the titration, the major product was the addition of three cyanide to dinitrophenyl ring that was shown as purple signals. The mechanism of this system was decided from the disappearance of all aromatic hydrogens belonging to that ring. To further understand the mechanism, HRMS spectra were taken with freshly added potassium cyanide to **DNBA** in ACN (c= 50 μM). After the addition of 1 equiv of CN^-, two different signals were obtained. One of them belonged to **DNBA**, while the other one had a mass of 313.0578 ($[M+H]^+$) that was consistent with the addition of cyanide to the dinitrophenyl fragment (**σ^H-complex 1**) (Supporting Information, **Figure S26**). When cyanide was increased to 5 equiv, beside **σ^H-complex 1** a new mass was encountered as 338.0531 ($[M+H]^+$) that consist of second cyanide addition to the ring (**σ^H-complex 2**) (Supporting Information, **Figure S27**). Even though different media, cyanide source (KCN and TBACN), and concentrations were used for the titration methods, the HR-MS (c = 50 μM, ACN) and the ^{1}H NMR (c= 10 mM, DMSO) results are compatible with the proposed mechanism (**Schemes 5** and **6**).

This article is protected by copyright. All rights reserved.

Accepted Manuscript

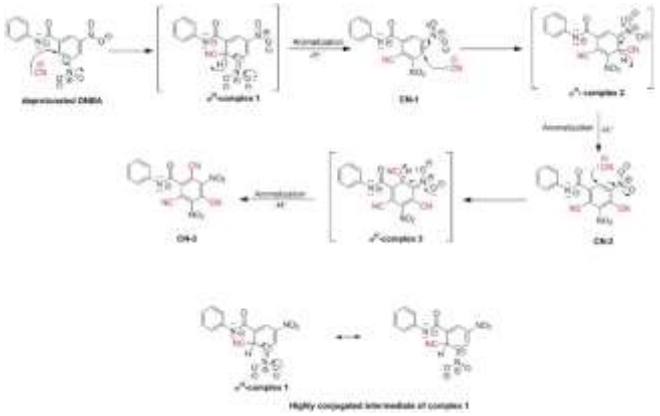

Scheme 6. Proposed mechanisms on cyanide additions to dinitrophenyl fragment.

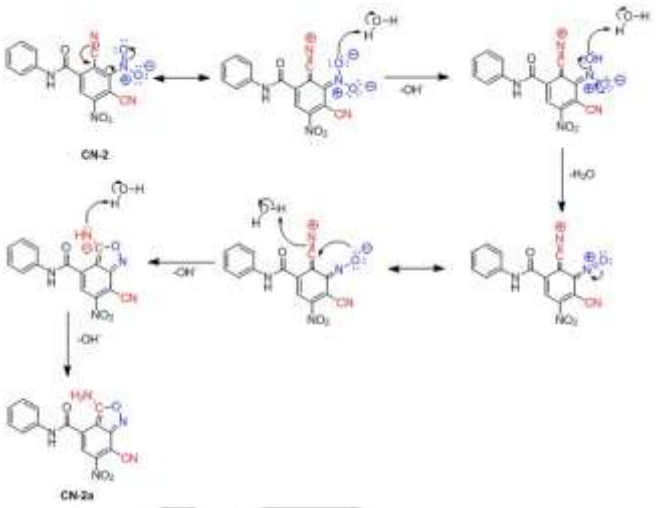

Scheme 7. Proposed mechanism on ring closing reaction via dicyano derivative of **DNBA**.

The plausible mechanism was shown in **Scheme 6**. Firstly, cyanide exhibited nucleophilic property and attacked at the ortho position of dinitrophenyl that is an electron-deficient system, leading to the intermediate **σ^H-complex 1**, followed by the departure of a proton through an eliminative pathway that produced the **CN-1** product.[15] The addition of cyanide causes the reaction to continue and a second a nucleophilic attack was at the para position of the dinitrophenyl ring (according to carbonyl), followed by an intermediate **σ^H-complex 2** and then the deprotonation of hydrogen to get **CN-2**. The last step was the third cyanide addition to the other ortho position of the dinitrophenyl ring (**σ^H- complex 3** then **CN-3**). The proposed mechanism by using ^{1}H NMR titration methods was also supported by the UV-vis titration method. While at the 250 nm absorption band belong to the deprotonation of the amide proton, at 400, 553 and 627 nm in ACN, the absorption bands can be attributed to mono, di and tri addition of cyanide to dinitrophenyl fragment, respectively. After the addition of cyanide, a new intermediate species (**σ^H-complex 1**, **2** and **3**) which have high conjugation in a ring can be obtained and absorption maxima shifted bathochromically because of the conjugation between the allylic anion and the dien/nitro or carbonyl and highly conjugated. In addition, the observed three absorption band may also be attributed to mono-, di- or tri cyanodinitro phenyl (see theoretical results, **Scheme 6**).

To support the reaction mechanism, the proposed structures need to isolate as pure products. To isolate of all the addition products, a few experiments were done and attempted to get pure products by using different purification methods (see experimental, syntheses and characterization parts). It is interesting that, while obtaining dicyano substituted **DNBA** derivatives, benzisoxazole derivative was obtained ring closing reaction via dicyano derivative of **DNBA** (**Scheme 7**). The product corresponding to benzisoxazole was characterized by X-ray crystallography (**Figure 1**-**2**, see Supporting Information).

Anion interaction study in Aqueous Medium

The applicability of the chemosensor **DNBA** was investigated for the determination of cyanide in the real sample, by the titration between the anions and the probe **DNBA** in aqueous solution. The interactions of the chemosensor with CN^- anion was first studied in DMSO/H_2O binary solvent mixtures varying from 9/1 to 1/9. The best response in terms of UV-vis and fluorescence spectra was obtained in a system containing DMSO/H_2O (8/2, v/v) (**Figure 11**). Upon addition of 20 equiv of all studied anions to an aqueous solution of **DNBA**, the chemosensor **DNBA** showed selectivity only towards CN^- anion besides competing anions such as F^-, AcO^- and $H_2PO_4^-$, also **DNBAM** showed same behavior towards CN^- in binary solvent mixtures (**Figures 11-13**, Supporting Information, **Figures S28-31**).

To determine the limit of detection (LOD), absorption titration of **DNBA** with CN^- was carried out by adding aliquots of micromolar concentration of TBACN in DMSO and DMSO/H_2O (8:2, v/v) mixture. The LOD was calculated using the equation: detection limit = 3σ/k, where σ is the standard deviation of blank, and k is the slope of the plot of the absorbances versus [CN^-]. The absorbance of **DNBA** at λ_{max} = 404 nm was measured 5 times in replicate, and the standard deviation of blank was determined. The absorbance (at 404 nm) was plotted vs. [CN^-] to obtain the slope (Supporting Information, **Figures S32** and **33**). The value of LOD obtained as 0.8 µM in DMSO, 1.5 µM in DMSO/ H_2O (8/2, v/v) binary solution. While the calculated LOD is lower than 2.7 µM which refers to WHO value for cyanide in aqueous solution.[16] Moreover, detection limits obtained in the present study are comparable with the reported values (Supporting Information, **Table S6**).

This article is protected by copyright. All rights reserved.

Accepted Manuscript

10.1002/ejoc.202000342

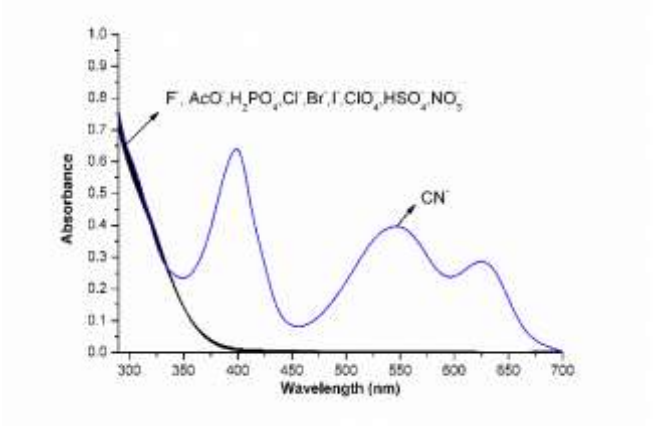

Figure 11. The absorption spectra of **DNBA** (*c*= 100 µM in DMSO/H_2O: 8/2, v/v) upon addition of 20 equiv of all used anions.

Figure 12. The photograph of **DNBA** (*c*= 100 µM) in DMSO/H_2O (the water contents were increased from left to right) (v/v) with 20 equiv of TBACN under ambient light (top) and UV lamp (λ_{ex} 365 nm, bottom).

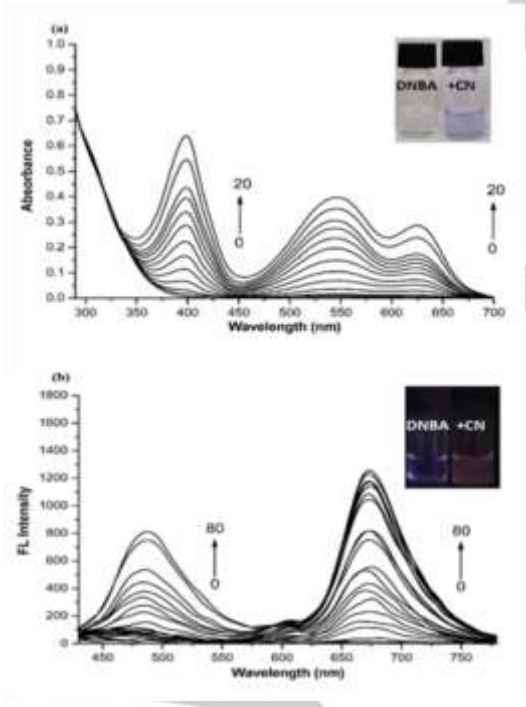

Figure 13. (a) Absorption spectra of **DNBA** (*c*= 100 µM in DMSO/H_2O: 8/2); (b) Emission spectra of **DNBA** (*c*= 50 µM in DMSO/H_2O: 8/2) after addition of 20 and 80 equiv of cyanide, respectively.

Application in real CN^- samples in tap water

The sufficient results obtained in DMSO/H_2O: 8/2 (v/v), for **DNBA**, encouraged us to put into practice the use of tap water, instead of distilled water. In this experiment, TBACN solved in tap water (50 µM) was used instead of TBACN in DMSO and fluorescence titration experiment was done. The results showed a turn-on in the fluorescence. **Figure 14** represents the response of **DNBA** upon the addition of 20 equiv of TBACN, and an intensive red fluorescence increment can be seen in the photograph (**Fig. 14**-inset). This result proved that the detection of CN^- ions can be realized using a simple UV lamp without any analytical devices.

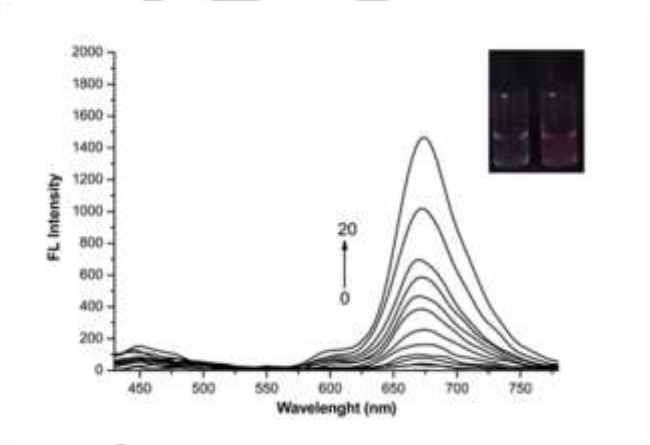

Figure 14. The emission spectra of tap water experiment (*c*= 50 µM in DMSO/Tap water: 8/2, v/v) upon the addition of 20 equiv of TBACN dissolved in tap water. Inset: photograph of **DNBA** (1 µM) in DMSO/Tap water (8/2, v/v) with 20 equiv of TBACN under UV lamp (λ_{ex}. 365 nm).

The usable colorimetric test strips for fast determination of CN^- could be important and useful for environmental samples. For this, especially inexpensive test strips can be produced by filter papers/TLC plates. In this study, the **DNBA** solution in ACN (1 mM) were dropped in TLC plate and dried in air. Cyanide solution in ACN (1 mM) were added one drop on this plate and the color change from colorless to blue was observed (**Figure 15**). This experiment reflects that the **DNBA**-based test strips can be proper detect CN^- in solutions without any other tools.

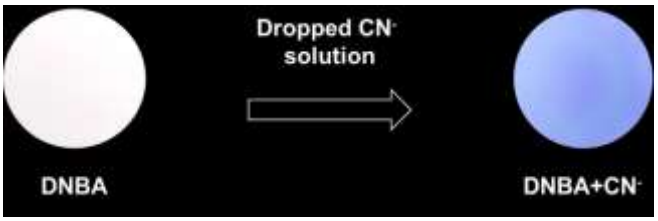

Figure 15. The photograph of the TLC plates loaded with **DNBA** were detected to sense CN^- in ACN solution with naked eye.

This article is protected by copyright. All rights reserved.

Accepted Manuscript

Theoretical results

To support the sensing mechanisms of **DNBA** with F^- and CN^-, the structural and electronic properties of DNBA and its adducts were obtained within the DFT calculations at B3LYP/6311+g(d,p) level. The optimized geometries of **DNBA** and its complexes formed via deprotonation with F^- and CN^- were shown in **Figure 16**. In the deprotonation process, F^- and CN^- interact with amide -NH proton and the distance N12-H13 changes significantly as seen in **Figure 16**. For **DNBA** and its fluoride or cyanide adducts formed via the deprotonation process, phenyl and amide were almost planar with the dihedral angle at about -177º. The dihedral angle between amide and dinitrophenyl ring was at about -156º. Upon interaction with F^- or CN^- via deprotonation process, there were no any geometrical changes, but the conjugation of the phenyl ring increases with the increase of the negative charge on nitrogen atom. The calculated absorption spectra of the deprotonated **DNBA** with F^- in DMSO have a peak at 318 nm with oscillator strength f=0.3986 and a broad peak at 494 nm with very small f value (f=0.0178) (**Table S7**), which are consistent with experimental results.

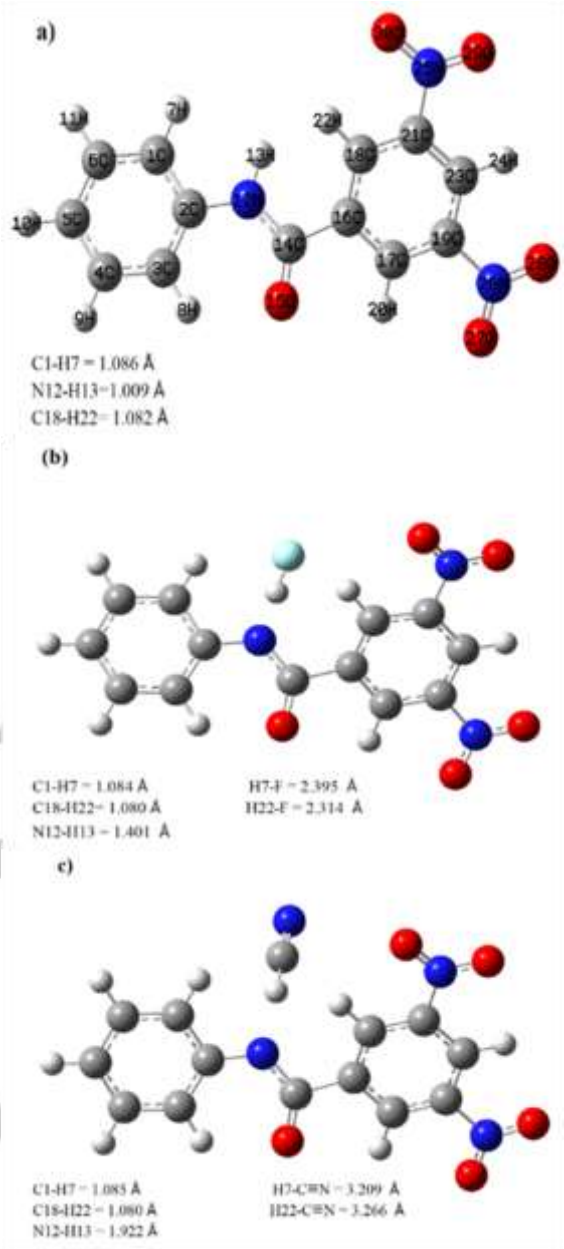

Figure 16. The optimized structures of a) **DNBA** and its complex formed via deprotonation with b) F^-, c) CN^-.

The complexes for the addition of F^- or CN^- given in **Scheme 4** and **6** were optimized in gas phase and the obtained geometries were illustrated in **Figure 17** and **Figure S34** (in Supporting Information). In case of addition CN^-, amide and dinitrophenyl ring became more planar than **DNBA** for **σ^H-complex 1** (the dihedral angle~173º) and for **CN-1**, **CN-2** and **CN-3** (the dihedral angle~180º) while it was the same with DNBA for **σ^H-complex 2** (the dihedral angle~149º), **σ^H-complex 3** (the dihedral angle~156º). Similar geometrical changes were also observed for the addition $^-$:CH_2CN adducts (Supporting Information, **Figure S34**). However, conjugations between the allylic anion and diene/nitro or carbonyl in σ^H-complexes and also conjugations in the aromatic cyano-substituted dinitrophenyl ring in adducts (**CN-1**, **CN-2**, **CN-3** or **ACN-1**, **ACN-2**) are expected to cause bathochromic shifts in the absorption spectra.

This article is protected by copyright. All rights reserved.

Accepted Manuscript

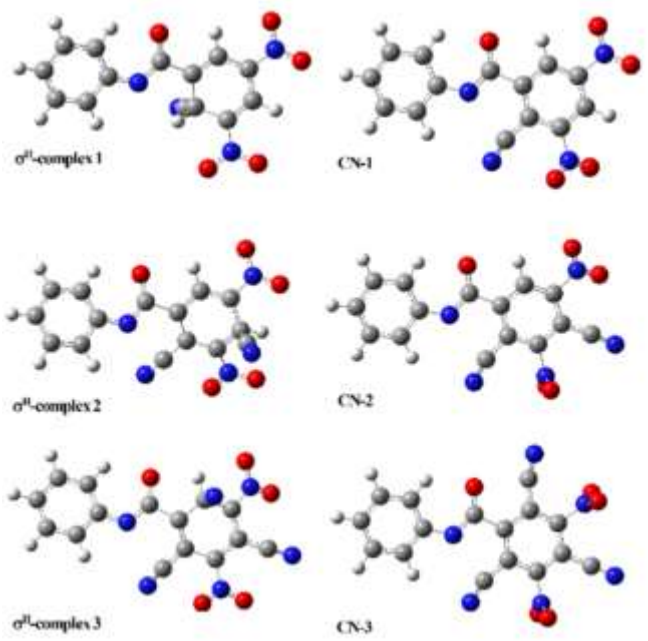

Figure 17. The optimized structures of the adducts formed via the addition of CN^- to **DNBA**.

In case of the addition of CN^- to the dinitrophenyl fragment, the peaks are observed at 401 nm and 478 nm for mono addition (**σ^H-complex 1**), at 425 nm and 525 nm for di addition **σ^H-complex 2**), at 494 nm for tri addition **σ^H-complex 3**). After the deprotonation of hydrogen in each σ^H -complexes, the absorption spectra obtained for **CN-1**, **CN-2** and **CN-3** have a main peak at 396 nm, 492 nm and 597 nm, respectively (**Table S8**). In addition, the obtained absorption maxima of the complexes of the $^-$:CH_2CN addition are consistent with the experimental results (**Table S7**). The comparison of the calculated and experimental data resulted that the peaks observed in the experimental spectrum can be attributed to the coexistence of different species.

Conclusion

In summary, **DNBA** was synthesized for the selective colorimetric and fluorimetric determination of cyanide anion in organic and aqueous solution. The proposed mechanism in the previously published study was improved and explained by spectroscopic titration analyses. The chemosensor **DNBA** showed a chromogenic and a fluorogenic selective response to CN^- against competing anions such as F^-, AcO^-, $H_2PO_4^-$ in DMSO and ACN. Three proposed sensing mechanisms named as deprotonation, nucleophilic aromatic substitution, and formation of benzisoxazole ring were confirmed by the UV-vis, fluorescence and ^{1}H NMR and mass spectroscopy techniques as well as X-ray crystallography. In addition, the experimental results were explained by the theoretical studies. **DNBA** showed that the detection of cyanide with LODs of 0.8 µM in DMSO, 1.5 µM in DMSO/H_2O (8:2, v/v) mixture, which was lower than those in WHO value for cyanide in aqueous solution. In addition, prepared colorimetric test strips with **DNBA** indicated a promising application of **DNBA** as a portable and fast strip for real-time naked-eye detection of CN^-. As a result, **DNBA** can be used to detect CN^- for environmental real water sample analysis with satisfactory results.

Experimental Section

Materials and reagents. The TBA salts of anions and all other reagents were purchased from Sigma-Aldrich. The solvents of analytical grade were purchased from Avra Chemicals and used without further purification.

General Information. All commercially available chemicals were reagent grade and used without further purification. Thin-layer chromatography (TLC) was used for monitoring the reactions using pre-coated silica gel 60 F254 plates. FT-IR spectra were recorded on a Mattson 1000 FT-IR spectrophotometer (Gazi University Department of Chemistry, Turkey) in KBr (v, in cm-1). NMR spectra were measured on a Bruker Avance III 400 MHz (^{1}H: 400 MHz, ^{13}C: 100 MHz) NaNoBay FT-NMR spectrometer at the Mersin University Advanced Technology Education, Research and Application Center (MEITAM), VARIAN (Agilent) MERCURY 400 MHz (Varian, Palo Alto, CA, USA) at a proton resonance frequency of 400 and 100 MHz for carbon at Ankara University Faculty of Pharmacy, and Bruker Avance 300 (^{1}H: 300 MHz, ^{13}C:75 MHz) spectrometers at 20 °C (293 K). Chemical shifts (δ) are given in parts per million (ppm) using the residue solvent peaks as reference relative to TMS. Coupling constants (J) are given in hertz (Hz). Signals are abbreviated as follows: broad. br; singlet. s; doublet. d; doublet-doublet. dd; doublet-triplet dt; triplet. t; multiplet. Elemental analysis was performed using a Thermo Scientific Flash 2000 at the Gazi University Department of Chemistry. The X-ray crystal structure data were collected at the Mersin University, MEITAM by a Bruker APEX-II charge-coupled device (CCD) diffractometer. High-resolution mass spectra (HRMS) were recorded at Gazi University Faculty of Pharmacy using electron ionization (EI) mass spectrometry (Waters-LCT-Premier-XE-LTOF (TOF-MS) instruments; in m/z (rel. %). The melting points were measured using the Electrothermal IA9200 apparatus. Absorption spectra were recorded on a Shimadzu 1800 spectrophotometer; fluorescence spectra were recorded on a Hitachi F-7000 fluorescence spectrophotometer.

Theoretical Methods

The geometries of the structures were optimized using Gaussian 09 package program[17] with Density Functional Theory (DFT) calculations at B3LYP/6311+g(d,p) level.[18] Frequency calculations performed on the optimized geometries confirm that the geometries correspond to local minima in a potential surface by the absence of imaginary frequency. The absorption spectrum was calculated using TD-DFT calculations at the same level. The solvent effect was considered using the integral equation formalism of the Polarizable Continuum Model (PCM).[19]

This article is protected by copyright. All rights reserved.

Accepted Manuscript

X-ray diffraction analysis

For the crystal structure determination, a single-crystal of the compound X was used for the data collection on a four-circle Rigaku R-AXIS RAPID-S diffractometer (equipped with a two-dimensional area IP detector). Graphite-monochromated Mo-Kα radiation (λ= 0.71073 Å) and oscillation scans technique with ∆w = 5º for one image were used for data collection. The lattice parameters were determined by the least-squares methods based on all reflections with $F^2 > 2\sigma$ (F^2). Integration of the intensities, correction for Lorentz and polarization effects and cell refinement were performed using CrystalClear (Rigaku/MSC Inc., 2005) software.[20] The structures were solved by direct methods using SHELXS-97[21] which allowed for the location of most of the heaviest atoms, with the remaining non-hydrogen atoms being located from different Fourier maps calculated from successive full-matrix least-squares refinement cycles on F^2 using SHELXL-97.[21] All non-hydrogen atoms were refined using anisotropic displacement parameters. Hydrogens attached to carbons were located at their geometric positions using appropriate HFIX instructions in SHELXL. The final difference Fourier maps showed no peaks of chemical significance. Crystal data for **CN-2a**: $C_{15}H_9N_5O_4$, crystal system, space group: monoclinic, $P2_1/c$; (no:14); unit cell dimensions: a = 9.959(4), b = 7.148(3), c = 19.758(5) Å, α= 90, β = 92.28(2), γ = 90º; volume; 1405.4(9) Å3, Z=4; calculated density: 1.528 g/cm^3; absorption coefficient: 0.116 mm-1; F(000): 664; θ-range for data collection 2.9-28.3º; refinement method: full-matrix least-squares on F^2; data/parameters: 3068/218; goodness-of-fit on F^2: 0.948; final R-indices [I > 2 σ (I)]: R1 = 0.076, wR2 = 0.183; largest diff. peak and hole: 0.199 and -0.210 e Å^{-3}.
Deposition **CCDC Number** 1980003 contains the supplementary crystallographic data for this paper. These data are provided free of charge via the joint CCDC/FIZ Karlsruhe deposition service www.ccdc.cam.ac.uk/structures.

Characterization data and synthetic procedures. *Synthesis of 3,5-dinitro-(N-phenyl)benzamide (**DNBA**)*; A solution containing aniline (1 mmol) and K_2CO_3 (1 mmol) in THF (5 mL) was cooled to 0 °C in an iced bath. To this solution, at 0 °C, 3,5-dinitrobenzoyl chloride (1 mmol) was slowly dropped. The temperature of the reaction mixture was raised to room temperature and continued to stir overnight. After that, water (20 mL) was added. The residue was filtered and crystallized with petroleum ether. Yield 75%, m.p. 233 °C, lit. m.p. 238.8[12]; FT-IR (cm^{-1}): 3280, 3103, 1652, 1630, 1599. ^{1}H NMR (DMSO-d_6, 300 MHz): δ 10.86 (s, 1H), 9.18 (d, *J* = 2.1 Hz, 2H), 9.01 (t, *J* = 2.1 Hz, 1H), 7.85 – 7.74 (m, 2H), 7.42 (dd, *J* = 8.5, 7.4 Hz, 2H), 7.20 (d, *J* = 7.4 Hz, 1H); ^{13}C NMR (DMSO-d_6, 75 MHz): δ 160.8, 147.7, 137.8, 137.0, 128.4, 127.6, 124.1, 120.7, 120.2. HRMS (TOF ES$^+$) (m/z), [M+H]$^+$ calcd for $C_{13}H_9N_3O_5$, 288.0576; found, 288.0593 and [M+H+CH_3CN]$^+$ calcd for $C_{13}H_9N_3O_5$, 329.0808; found, 329.0845. Elemental analysis: anal. calc. for $C_{13}H_9N_3O_5$; C, 54.36; H, 3.16; N, 14.63; found: C, 54.48; H, 3.26; N, 14.24.

*Synthesis of N-methyl-3,5-dinitro-N-phenylbenzamide (**DNBAM**)*; A solution containing *N*-methylaniline (1 mmol) and K_2CO_3 (1 mmol) in THF (5 mL) was cooled to 0 °C in an iced bath. To this solution, at 0 °C, 3,5-dinitrobenzoyl chloride (1 mmol) was slowly dropped. The temperature of the reaction mixture was raised to room temperature and continued to stir overnight. After that, water (20 mL) was added. The residue was filtered and crystallized with petroleum ether. Yield 70%, m.p. 160 °C; ^{1}H NMR (DMSO-d_6, 400 MHz): δ 8.69 (t, *J* = 2.2 Hz, 1H), 8.43 (s, 2H), 7.33 (d, *J* = 7.5 Hz, 2H), 7.29 (t, *J* = 7.7 Hz, 2H), 7.19 (t, *J* = 7.1 Hz, 1H), 3.42 (s, 3H). ^{13}C NMR (DMSO-d_6, 100 MHz): δ 165.5, 147.8, 143.7, 139.7, 129.9, 128.9, 127.8, 127.7, 119.6. HRMS (TOF ES$^+$) (m/z), [M+H]$^+$ calcd for $C_{14}H_{11}N_3O_5$, 302.0777; found, 302.0769.

*Synthesis of 3-amino-7-cyano-6-nitro-N-phenylbenzo[c]isoxazole-4-carboxamide (**CN-2a**)*

Path 1: To a stirred solution of the **DNBA** (1 mmol) in DMSO (15 mL) was added a solution of tetrabutylammonium cyanide (3.0 mmol) in (5 mL) DMSO at room temperature and the reaction mixture was stirred for 2 h. After completion of the reaction, 50 mL of deionized water was added and the mixture was extracted three times with ethyl acetate. The crude mixture was purified by column chromatography (ethyl acetate: hexane / 1:4) and the pure product was obtained as dark crystals in 35% yield. Furthermore, 2,4,6-tricyano-3,5-dinitro-*N*-phenylbenzamide (**CN-3**) was obtained with a trace amount (yield less than 1%) after chromatographic purification.
Path 2: To a stirred solution of the **DNBA** (1.0 mmol) in DMSO (16 mL) was added a solution of potassium cyanide (3.0 mmol) in H_2O (4 mL) at room temperature and the reaction mixture was stirred for 96 h, but the reaction was not complete. Then, 50 mL of deionized water was added and the mixture was extracted three times with ethyl acetate. The crude mixture was purified by column chromatography (ethyl acetate:hexane/1:4) and the pure product was obtained as dark crystals in 8% yield.
m.p. 219 °C; FT-IR (cm^{-1}): 3386, 3273, 3225, 2233, 1981, 1659, 1616, 1595. ^{1}H NMR (DMSO-d_6, 400 MHz): δ 10.99 (s, 1H), 9.02 (s, 2H), 7.90 (s, 1H), 7.77-7.75 (m, 2H), 7.44-7.40 (m, 2H), 7.23-7.19 (m, 1H); ^{13}C (DMSO-d_6, 100 MHz): δ 169.1, 162.7, 156.3, 153.0, 137.63, 137.58, 128.7 (2 x C), 125.1, 121.6 (2 x C), 112.2, 111.2, 99.5, 92.1. HRMS (TOF ES$^+$) (m/z), [M+H]$^+$ calcd for $C_{15}H_{10}N_5O_4$, 324.0733; found, 324.0727.
^{1}H NMR data for (**CN-3**): ^{1}H NMR (DMSO-d_6, 400 MHz): δ 7.76 - 7.63 (m, 5H).

Acknowledgements

This research was supported by Gazi University. The numerical calculations reported in this paper were fully performed at TUBITAK ULAKBIM, High Performance and Grid Computing Center (TRUBA resources).

Keywords: Chemosensor • Colorimetric/Fluorimetric chemosensor • Selective cyanide detection • Nucleophilic aromatic substitution of hydrogen (NASH) • S_N^H • Benzisoxazole

[1] a) B. Valeur, F. Badaoui, E. Bardez, J. Bourson, P. Boutin, A. Chatelain, I. Devol, B. Larrey, J. Lefevre, A. Soulet, *NATO ASI series. The Netherlands: Kluwer: Dordrecht* **1997**; b) F. P. Schmidtchen, M. Berger, *Chem. Rev.* **1997**, *97*, 1609-1646; c) P. D. Beer, *Acc. Chem. Res.* **1998**, *31*,

This article is protected by copyright. All rights reserved.

Accepted Manuscript

71-80; d) J. Atwood, J. Steed, A. Bianchi, E. Garcia-Espana, *BiachiK, A., Bowman-James, K., Garcia-Espana, E., Eds* **1997**; e) J.-M. Lehn, *Supramol. Chem. Vol. 1*, Vch, Weinheim Germany, **1995**; f) H. Singh, K. Tiwari, R. Tiwari, S. K. Pramanik, A. Das, *Chem. Rev.* **2019**, *119*, 11718-11760.

[2] a) H. Komatsu, T. Miki, D. Citterio, T. Kubota, Y. Shindo, Y. Kitamura, K. Oka, K. Suzuki, *J. Am. Chem. Soc.* **2005**, *127*, 10798-10799; b) N. Kaur, S. Kumar, *ChemComm* **2007**, 3069-3070; c) M. Schmittel, H. Lin, *Inorg. Chem.* **2007**, *46*, 9139-9145; d) D. Y. Lee, N. Singh, D. O. Jang, *Tetrahedron Lett.* **2010**, *51*, 1103-1106; e) M. Yuan, W. Zhou, X. Liu, M. Zhu, J. Li, X. Yin, H. Zheng, Z. Zuo, C. Ouyang, H. Liu, *The J. Org. Chem.* **2008**, *73*, 5008-5014; f) S. Wang, G. Men, L. Zhao, Q. Hou, S. Jiang, *Sens. Actuators B: Chem.* **2010**, *145*, 826-831; g) K. L. Kirk, in *Biochemistry of the Elemental Halogens and Inorganic Halides*, Springer, **1991**, pp. 19-68; h) I. Yahaya, Z. Seferoglu, in *Photochemistry and Photophysics Fundamental Applications* IntechOpen, **2018**; i) J. Westley, B. Vannesland, E. Conn, C. Knowles, F. Wissing, London: Academic Press Inc, **1981**; j) A. Ghosh, B. Ganguly, A. Das, *Inorg. Chem.* **2007**, *46*, 9912-9918.

[3] a) M. Kleerekoper, *Endocrin. Metab. Clin.* **1998**, *27*, 441-452; b) D. Briancon, P. Meunier, *Orthop. Clin. North Am.* **1981**, *12*, 629; c) D. A. Jose, P. Kar, D. Koley, B. Ganguly, W. Thiel, H. N. Ghosh, A. Das, *Inorg. Chem.* **2007**, *46*, 5576-5584.

[4] C. K. Mathews, K. Van Hold, Cumming Publishing Company, Inc, **1990**.

[5] a) J. L. Sessler, Gale P. A., Cho, W. S., *Anion Receptor Chemistry* **2006**, 1-26; b) A. Paul, M. Perween, S. Saha, D. N. Srivastava, A. Das, *Phys. Chem. Chem. Phys.* **2015**, *17*, 26790-26796.

[6] a) S. K. Kim, J. H. Bok, R. A. Bartsch, J. Y. Lee, J. S. Kim, *Org. Lett.* **2005**, *7*, 4839-4842; b) D. Saravanakumar, S. Devaraj, S. Iyyampillai, K. Mohandoss, M. Kandaswamy, *Tetrahedron Lett.* **2008**, *49*, 127-132; c) Y. Wu, X. Peng, J. Fan, S. Gao, M. Tian, J. Zhao, S. Sun, *J. Org. Chem.* **2007**, *72*, 62-70; d) P. Ashokkumar, V. T. Ramakrishnan, P. Ramamurthy, *Chem. Eur. J.* **2010**, *16*, 13271-13277.

[7] a) Y. M. Chung, B. Raman, D.-S. Kim, K. H. Ahn, *ChemComm.* **2006**, 186-188; b) P. Anzenbacher, D. S. Tyson, K. Jursíková, F. N. Castellano, *J. Am. Chem. Soc.* **2002**, *124*, 6232-6233; c) S. Saha, A. Ghosh, P. Mahato, S. Mishra, S. K. Mishra, E. Suresh, S. Das, A. Das, *Org. Lett.* **2010**, *12*, 3406-3409.

[8] a) J. L. Sessler, D.-G. Cho, *Org. Lett.* **2008**, *10*, 73-75; b) Y. Sun, Y. Liu, W. Guo, *Sens. Actuators B: Chem.* **2009**, *143*, 171-176; c) Y. Shiraishi, K. Adachi, M. Itoh, T. Hirai, *Org. Lett.* **2009**, *11*, 3482-3485; d) S.-H. Kim, S.-J. Hong, J. Yoo, S. K. Kim, J. L. Sessler, C.-H. Lee, *Org. Lett.* **2009**, *11*, 3626-3629; e) S. Park, H.-J. Kim, *ChemComm.* **2010**, *46*, 9197-9199; f) Y.-K. Yang, J. Tae, *Org. Lett.* **2006**, *8*, 5721-5723; g) F. García, J. M. García, B. García-Acosta, R. Martínez-Máñez, F. Sancenón, J. Soto, *ChemComm.* **2005**, 2790-2792; h) H. Agarwalla, M. Gangopadhyay, D. K. Sharma, S. K. Basu, S. Jadhav, A. Chowdhury, A. Das, *J. Mater. Chem. B* **2015**, *3*, 9148-9156.

[9] a) K. P. Divya, S. Sreejith, B. Balakrishna, P. Jayamurthy, P. Anees, A. Ajayaghosh, *ChemComm.* **2010**, *46*, 6069-6071; b) X. Lou, L. Zhang, J. Qin, Z. Li, *ChemComm.* **2008**, 5848-5850; c) Z. a. Li, X. Lou, H. Yu, Z. Li, J. Qin, *Macromolecules* **2008**, *41*, 7433-7439.

[10] a) Ö. Şahin, Ü. Ö. Özdemir, N. Seferoğlu, B. Aydıner, M. Sarı, T. Tunç, Z. Seferoğlu, *Tetrahedron* **2016**, *72*, 5843-5852; b) B. Aydıner, *J. Photochem. Photobiol. A* **2019**, *382*, 111916; c) M. Chemchem, I. Yahaya, B. Aydıner, O. Doluca, N. Seferoğlu, Z. Seferoğlu, *Sens. Actuators B: Chem.* **2020**, *305*, 127316.

[11] a) Z. Xu, X. Chen, H. N. Kim, J. Yoon, *Chem. Soc. Rev.* **2010**, *39*, 127-137; b) M. Cametti, K. Rissanen, *ChemComm.* **2009**, 2809-2829; c) J. Ma, P. K. Dasgupta, *Anal. Chim. Acta* **2010**, *673*, 117-125; d) P. A. Gale, *Chem. Soc. Rev.* **2010**, *39*, 3746-3771; e) Y. Chung, K. H. Ahn, *J. Org. Chem.* **2006**, *71*, 9470-9474; f) S. Erdemir, S. Malkondu, *Talanta* **2020**, *207*, 120278; g) P. Das, S. Saha, M. Baidya, S. K. Ghosh, A. Das, *ChemComm.* **2013**, *49*, 255-257.

[12] D.S. Kim, Y.M. Chung, M. Jun, K. H. Ahn, *J. Org. Chem.* **2009**, *74*, 4849-4854.

[13] a) M. Makosza, K. Wojciechowski, *Chem. Rev.* **2004**, *104*, 2631-2666; b) M. Makosza, *Chem. Soc. Rev.* **2010**, *39*, 2855-2868; c) T. Okamoto, H. Takahashi, Chem. Pharm. Bull. 1968, 16, 1700-1704; d) T. Okamoto, H. Takahashi, Chem. Pharm. Bull. 1971, 19, 1809-1814; e) T. Okamoto, H. Takahashi, H. Takayama, T. Kitagawa, M. Ikeda, Chem. Pharm. Bull. 1969, 17, 140-144; f) V. N. Charushin, O. N. Chupakhin, Mendeleev Commun., 2007, 17, 249–254.

[14] J. H. Clark, *Chem. Rev.* **1980**, *80*, 429-452.

[15] a) L. Chen, C. Fu, Z. Li, T. Zhu, X. Chen, C. Gao, T. Wang, W. Pang, C. Liu, *Tetrahedron Lett.* **2020**, 151656; b) M. G. Choi, N. Y. Kim, Y. J. Lee, S. Ahn, S. K. Chang, *ChemComm.* **2019**, *55*, 11398-11401.

[16] O. M. D. l. Sante, W. H. Organization, W.W. programme, W. H. O. Staff, S. O. Zdrowia, WHO, *Guidelines for drinking-water quality, Vol. 1*, World Health Organization, **2004**.

[17] M. J. Frisch, G. W. Trucks, H. B. Schlegel, G. E. Scuseria, M. A. Robb, J. R. Cheeseman, et al. Gaussian 09, revision C.01. Wallingford CT: Gaussian, Inc.; **2010**.

[18] a) C. Lee, W. Yang, R. G. Parr, *Phys. Rev. B* **1988**, *37*, 785; b) A. D. Becke, J. *Chem. Phys*, *98*, 5648; c) P. C. Hariharan, J. A. Pople, *Theor. Chim. Acta.* **1973**, *28*, 213-222.

[19] a) J. Tomasi, R. Cammi, B. Mennucci, C. Cappelli, S. Corni, *Phys. Chem. Chem. Phys.* **2002**, *4*, 5697-5712; b) M. Cossi, V. Barone, *J. Chem. Phys.* **2001**, *115*, 4708-4717.

[20] Rigaku/MSC, Inc., 9009 New Trails Drive, TheWoodlands, TX 77381.

[21] G. M. Sheldrick, *Acta Crystallogr., Sect. A: Found. Crystallogr.* **2008**, *64*, 112-122.

Accepted Manuscript

This article is protected by copyright. All rights reserved.

10.1002/ejoc.202000342

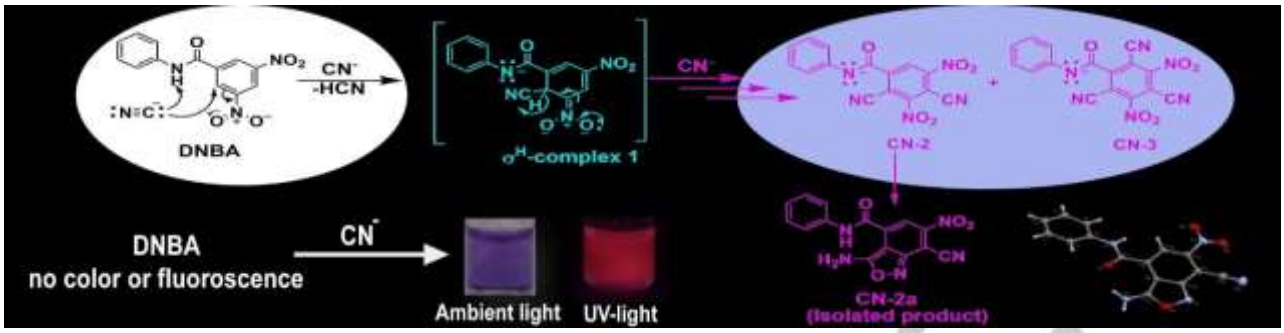

WILEY-VCH

Accepted Manuscript

This article is protected by copyright. All rights reserved.